Iranian Journal of Materials Science and Engineering, Vol. 20, Number 3, September 2023
RESEARCH PAPER

A Systematic Study on Mechanical Properties of CNT Reinforced HDPE Composites Developed Using 3D Printing

Deepak Jagannathan[1,*], Hiriyannaiah Adarsha[1], Keshavamurthy Ramaiah[2], Ramkumar Neralur Prabhu[1]

* *deepakiyer31@gmail.com*

[1] Department of Mechanical Engineering, Faculty of Engineering and Technology, Jain Global Campus, Bengaluru 562 112, India;
[2] Department of Mechanical Engineering, Dayananda Sagar College of Engineering, Bangalore, India;

Received: April 2023 **Revised: August 2023** **Accepted: August 2023**
DOI: 10.22068/ijmse.3231

Abstract: *Several extensive researches are being carried out in the field of 3D printing. Polymer matrices, such as High-Density Polyethylene (HDPE), are less explored particularly on the microstructure and mechanical properties of HDPE composites developed via the Fused Deposition Modelling (FDM) process. Very scarce amount of work is devoted to studying HDPE's reinforced with carbon nano-tubes (CNT's). In the present work, we report on the mechanical properties of HDPE composites prepared via the FDM process. Varying proportions of CNTs (0.5, 1, 1.5, and 2%) are used as reinforcements. It is found that increasing CNT content enhances impact and tensile strength, with HDPE/2.0%CNT outperforming pure HDPE by approximately 71.6% and 25.4%, respectively. HDPE/2.0%CNT composite also showed Young's modulus approximately 49.2% higher than pure HDPE. According to fracture analysis, pure HDPE failed near ductile, whereas composites failed brittle. CNTs occupy the free positions in the polymeric chains, and their tendency to restrict chain mobility causes HDPE to lose ductility and begin to behave brittlely. The use of CNTs as reinforcement successfully improved the mechanical properties of HDPE.*

Keywords: *Fused deposition modelling; Carbon nanotubes; Mechanical properties; Fracture.*

1. INTRODUCTION

Additive manufacturing, also known as 3D printing, has attracted considerable interest from academia and industry. The ability to easily print complex 3D objects layer by layer is the main feature of 3D printing. However, a 3D CAD model and CAM software, which is used to slice the model and aid the printing path, are required to complete this task [1, 2]. Unlike traditional techniques, which require the creation of a new tool, jig, or mould for new products or design changes, 3D printing does not have such constraints. This technique is used to make a variety of products in industries such as automotive, medical, architectural, toy, energy storage, and aerospace. According to the American Society for Testing and Materials (ASTM) standards, there are seven major categories of 3D printing. In comparison to traditional techniques, 3D printing offers greater design flexibility, faster prototyping, the ability to fabricate complex dimensions and geometries, the elimination of the machining process, and physical morphology tailoring [3-6]. Fused deposition modelling (FDM) is a popular 3D printing technique that entails melting material, extrusion, and layer-by-layer deposition to achieve the desired shape and size. It is also known as fused filament fabrication because the material being melted is usually in the form of filament that is rolled on a spool (FFF). FDM is well-known for printing large and rigid objects with ease and at the lowest cost-to-size ratio [7-10]. FDM has been used to print a wide range of polymers, including ABS, nylon, polylactic acid (PLA), polyphenylsulfone, polyethylene terephthalate glycol (PETG), and polycarbonate-based objects [11-14].

HDPE is a thermoplastic that is commonly used in the production of water bottles, chemical containers, light-duty tanks, outdoor cabinetry, pipe systems, and marine construction parts [15]. This polymer's popularity stems primarily from its lightweight and high strength, as well as the fact that it does not absorb liquids, has high chemical stability, and is non-toxic. Although ABS and PLA polymers were popular as FDM filament materials, printing HDPE parts took some time and effort. Poor interlayer adhesion, shrinkage susceptibility, and warpage are just a few of the issues that limit the use of FDM 3D printing for HDPE. Studies have reported 3D printing of neat HDPE, blends, and fiber/particle-

[DOI: 10.22068/ijmse.3231]

reinforced HDPE composites. Schirmeister et al [16] reported the development of HDPE specimens using a twin-screw extruder and the FFF technique, for example. Considering the drawbacks of HDPE, the authors optimised the printing parameters by varying the extrusion rate, nozzle temperature, nozzle diameter, build plate material, and temperature. With no void formation or warpage, the mechanical properties of the FFF-printed HDPE were comparable to those of the injection moulded counterpart. In an intriguing study, recycled HDPE was put through a series of characterization tests to determine its suitability as a 3D printing material [17]. A variety of HDPE products were cleaned, dried, shredded, and extruded to create 3D printing filaments for FFF printers. The extruded filaments exhibited thermal stability, water rejection, and mobility. Gudadhe et al [18] reported similar work in which waste HDPE was combined with low-density polyethylene and printed using an FFF printer. Furthermore, FEM simulations were performed to identify the source of stresses generated during the printing process. Kumar et al. [19] investigated the mechanical properties of recycled HDPE reinforced with Fe particles for use as filament materials in FDM printers.

Based on the melt flow index, low porosity content, and dense structure, the optimum Fe content that could be added to HDPE was 10%. These studies have provided several insights into HDPE FDM 3D printing and how to overcome its limitations.

Over the last few decades, the use of nanomaterials as reinforcement for polymer matrices has grown dramatically. Carbon nanostructures with unique mechanical and physical properties, such as carbon nanotubes, carbon black, graphene, and fullerene, have piqued the interest of researchers. Carbon nanotubes (CNTs) have extremely high strength and elastic modulus values of 63 - 126 GPa and 0.915 - 1 TPa, respectively [20-23]. Because of these properties, carbon nanotubes are ideal reinforcing agents for strengthening polymer matrices. However, the degree of strengthening is highly dependent on CNT dispersion, bonding, and orientation, making full utilisation of CNT strength and stiffness difficult. To summarise the most recent developments, many review articles on CNT-reinforced polymer composites have been written. The topics covered in these review articles [24-26] range from composite fabrication techniques to mechanical, thermal, and electrical properties. The development of polymer composites with CNT using FDM, on the other hand, is still in its early stages, and the various properties of these composites are being studied. Ye et al [27] reported on the mechanical and electrical properties of CNT-reinforced thermoplastic polyimide composites. The effect of CNT content was investigated, and it was discovered that the tensile strength, bending strength, and conductive resistivity of composites decreased as CNT content increased. Incomplete crystallisation, high internal stress, and internal defects caused by insufficient extrusion pressure were the main causes of poor properties. In another paper, Sezer and Eren [28] reported the development of MWCNT-reinforced ABS parts using the FDM 3D printing technique. The tensile strength and Young's modulus of nanocomposites were found to increase with increasing CNT content. CNT functionalization improved bonding and dispersion in the ABS matrix, resulting in improved properties. Loading CNTs above 10%, on the other hand, resulted in a decrease in properties due to CNT agglomeration. Yang et al [29] investigated the effect of carbon nanotubes (CNTs) on the melt flow rate and mechanical properties of PLA composites. The melt flow rate decreased as CNT content increased, implying an increase in viscosity due to the nucleation effect between PLA and CNT. Composite tensile and flexural strength increased as a result of effective load transfer to CNT and improved layer adherence. Finally, due to the content, dispersion, and orientation of CNTs, defects can form during the printing process, which must be avoided. Underflow caused by an increase in melt viscosity can increase the number of defects between the roads/rasters or clog the nozzle. Such issues must be addressed in CNT-reinforced polymer matrices to achieve better mechanical properties.

These studies discovered that polymer composites containing CNTs performed better overall. This research focuses on developing HDPE-based polymer nanocomposites using FDM technology by reinforcing CNT which was earlier extensively studied using more conventional methods. The effect of CNT on the surface roughness, tensile, and impact properties of HDPE composites created

[DOI: 10.22068/ijmse.3231]

using FDM 3D printing is studied.

2. EXPERIMENTAL PROCEDURES

2.1. Materials

Carbon nanotubes procured from local vendor (Purity: ~99%, Outer diameter: ~10-30 nm, length: ~10 μm, Ad-Nano Technologies Pvt. Ltd., India) were used as reinforcement. On the other hand, high-density polyethylene (Density: 0.947 g/cm^3, Polyshakti Polymers, India) in the form of pellets was used as matrix material. The photographs of both materials are presented in the Figs. 1 (a) and (b). SEM and EDX of the procured CNT samples are shown in Figs. 1 (c) and (d) respectively.

2.2. Fabrication

For the preparation of the composites, 1000 ml of dichloromethane solvent was combined with the starting materials in known amounts. The entire mixture was thoroughly mixed in a magnetic stirrer at room temperature. The stirring process was continued for approximately 120 minutes, after which the solvent was removed by placing the composite slurry in a 100°C oven. After drying, the mixture was fed into a compounding machine and formed into wire.

These wires were formed into small pellets before being extruded with a twin screw extruder. To improve diameter tolerances and smooth extrusion, a temperature of 190°C was used. The diameter of the filament was kept constant by controlling the drawing speed of the extruder. Photographs of filament drawn with a twin screw extruder are shown in Figs. 2 (a) and (b). The various 3D parts were printed using an FFF printer (Make: Praman 3D printer, Global 3D labs, India). Figs. 2 (c) and (d) shows 3D printed tensile and impact test specimens. Table 1 and 2 displays the parameters used to print the parts and specifications of the 3D printer used respectively.

2.3. Testing

The density of each sample was first determined using the Archimedes principle. Using a surface roughness tester, the surface roughness of FDM 3D-printed samples was then analysed (Make: Miyu M35, India). For this purpose, 10×10×20 mm (length, width & thickness) samples were fabricated, and roughly three measurements were taken for each composition.

The arithmetic mean roughness was used to measure the surface roughness (Ra).

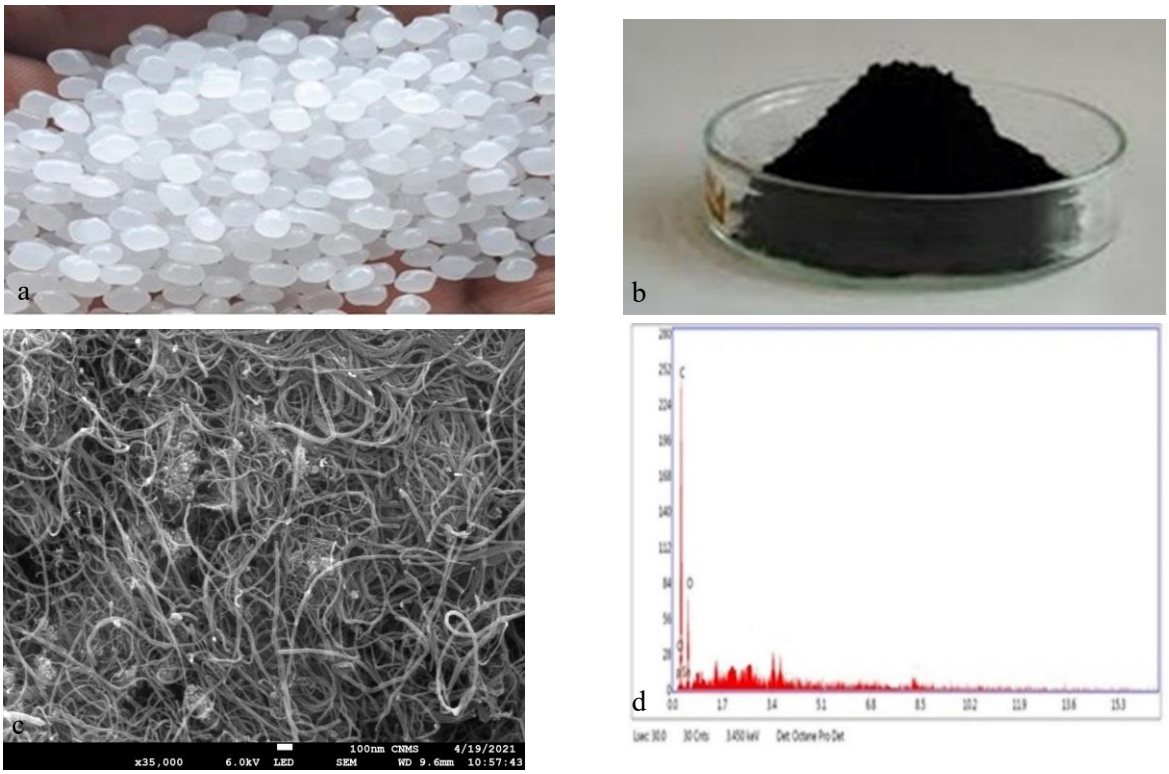

Fig. 1. (a) & (b): HDPE pellets and CNT powder, (c) and (d): SEM & EDX of CNT respectively.

[DOI: 10.22068/ijmse.3231]

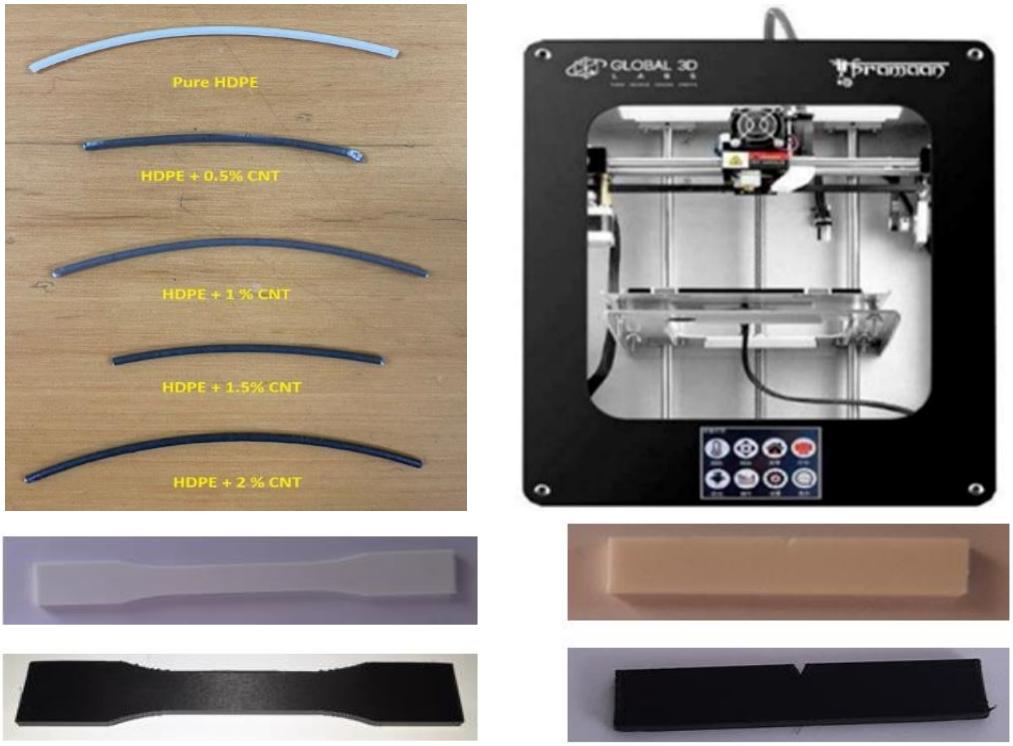

Fig. 2. (a) Photographs of filament drawn with a twin screw extruder (b). FFF printer used to print the various 3D parts (c) Tensile Test Specimen of Pure HDPE and HDPE + 2% CNT respectively (d) Impact Test Specimen of Pure HDPE and HDPE + 2% CNT.

Table 1. Parameters opted for filament extrusion and printing parts using FFF.

Filament Fabrication by Extrusion		**Printing parameters using FFF**	
Parameters	**Value**	**Parameters**	**Value**
T Zone 1	190°C	Build plate temperature	60°C
T Zone 2	200°C	Nozzle temperature	240°C
T Zone 3	200°C	Printing speed	25 – 100 mm/s
T Zone 4 / Nozzle	190°C	Layer thickness	0.1 mm
Speed of rotation	20 rpm	Line width	0.8 mm
Dosage	0.5 kg/hr	Filling pattern	Lines

Table 2. Technical specifications of FDM printer.

Parameters	**Value**
Technology	Fused Deposition Modelling
Print Size	160mm * 160mm * 180mm
Print Resolution	0.1 mm/100 Microns
Hot-end Type	Single Extruder
Nozzle-Type	Brass
Nozzle Maximum Temperature	260°C
Maximum Bed Temperature	100°C
Working Ambient Temperature	15-40°C
Connectivity	SD-Card/USB
Power	Input Voltage: 220 V, 50Hz Input Current : 5-6 Amp.

On FDM 3D printed samples prepared in accordance with ASTM D638 and D4812, standard mechanical properties tests, such as tension and impact tests, were conducted. The tensile test was conducted on a 60-tonne-capacity universal testing machine (Make: FIE Pvt. Ltd.,

[DOI: 10.22068/ijmse.3231]

India). All tests were conducted with a strain rate of 2 mm/s at room temperature. The average of the three samples tested for each composition is displayed here. The Izod impact test was conducted with an impact tester (Make: FIE Pvt. Ltd., India) equipped with a 300 J hammer and a 5 m/s pendulum speed at impact. Approximately three tests were conducted for each composition, and the value presented here is the mean of these three tests. The dispersion of CNTs in the HDPE matrix and fracture surfaces after tensile testing were investigated using a scanning electron microscope (Make: Tescan Vega3, India).

3. RESULTS AND DISCUSSION

3.1. Microstructure Analysis

CNT dispersion in the HDPE matrix, as well as the presence of any printing defects, have a significant impact on mechanical properties. SEM characterization was performed to examine the dispersion of CNTs and the quality of FDM 3D printed samples, and the representative results are shown in Figs. 3 (a-h). The CNTs are uniformly dispersed in the matrix and protrude out of the HDPE matrix, as seen in the HDPE/0.5%CNT composite (Fig. 3 (a)). In this region of the composite, there were no visible CNT agglomerates. Because there was no gap between the CNTs and the HDPE matrix, the bonding appeared to be strong. Because there were no bare surfaces on the CNTs, the interface appears to be continuous with proper matrix filling around it. Because the extruder could shear CNT aggregates, the low CNT content in this composite favoured better dispersion. Because of the twin screw extruder's ability to orient CNTs in the direction of extrusion, the orientation of the CNTs was discovered to be in the direction of deposition. If a specific orientation is not obtained during the filament extrusion process, obtaining it during FDM 3D printing is difficult. In this case, the ability to achieve specific orientation is due to the synergistic effect of both the filament extrusion and printing processes. In their work on 3D-printed CNTs/PLA composites, Zhou et al [30] made a similar observation. Many carbon nanotubes were observed to extend along the printing direction, indicating that the preferred orientation is possible in 3D printing. The EDAX analysis, as shown in Fig. 3 (b), confirmed the presence of CNT by displaying a C peak in the spectrum, as well as some other impurities. Like the previous case, the HDPE/1.0%CNT composite had a few CNTs protruding from the HDPE matrix (see Fig. 3 (c)). Bonding is also quite good in this case, with no interface defects and no CNT agglomeration observed. It should be noted that the uniform dispersion obtained for small CNT contents of 0.5% and 1.0% is especially significant. This is because many references have reported agglomeration in CNT nanocomposites containing 0.5% to 1.0% CNT [31,32]. Although no specific reason for the formation of CNT bundles was given, it did highlight practical limitations in achieving a higher level of dispersion using melt compounding. CNT agglomeration is generally caused by the van der Waals force between the CNTs. Pan et al [33] discovered CNT agglomeration in PLA composites after 3D printing. The formation of printing defects and surface roughness are two major aspects of printing quality that must be considered. All the composites were free of visible flaws and had excellent layer bonding. Although it is difficult to quantify surface roughness using SEM micrographs, it is clear that they appear rough. The surface of FDM 3D printing is not as smooth as expected, but the roughness is not significant. Because all of the printing parameters were held constant while the CNT was varied, the surface quality is heavily influenced by the CNT. The surface appears to be smoothing out in terms of CNT content, as shown in Fig. 3 (a) and (c). The surface of higher CNT content reinforced HDPE composites revealed several CNT edges protruding from the matrix (see Fig. 3 (e) and (g)). A closer look at these edges reveals that the bonding between the CNT and matrix was quite good, which will help with load transfer during tensile or impact loading. Aggregation is a common problem in the case of nanosized reinforcements, resulting in discontinuities and inhomogeneities in the composites. These aggregates are frequently characterised by poor matrix bonding and serve as stress concentrators. The absence of CNT agglomerates as CNT content increases is the main feature of these micrographs. The chosen extrusion and FDM printing parameters were able to disperse the aggregates uniformly by shearing them.

[DOI: 10.22068/ijmse.3231]

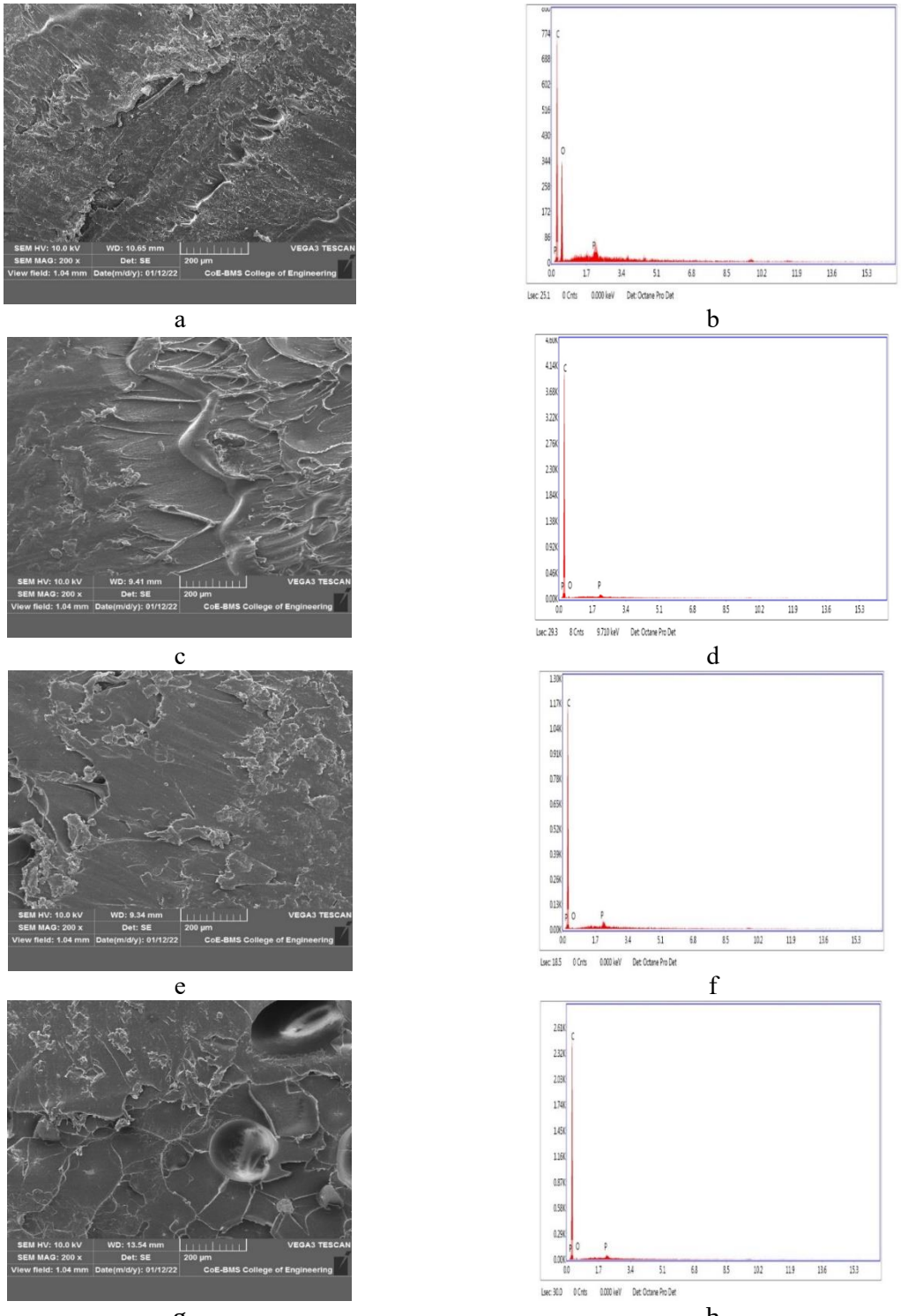

Fig. 3. SEM micrographs and respective EDAX of a,b) 0.5%, c,d) 1.0%, e,f) 1.5% and g,h) 2.0% CNT reinforced HDPE composites

When compared to other studies that found an increase in CNT agglomerate with respect to CNT content and discovered that the process parameters used were unable to shear the CNT aggregates [33,34], this is an intriguing finding. Few CNTs seen in the micrographs were not damaged during the mixing or printing processes, such as kinking or breaking of CNT walls. This

[DOI: 10.22068/ijmse.3231]

broadens the application of FDM 3D printing for the creation of HDPE/CNT composites. Furthermore, as shown in Figs. 3 (f) and (h), the EDAX analysis revealed a sharp and high-intensity C peak, confirming the presence of CNTs as well as some other impurities formed during the mixing process.

3.2. Surface Roughness and Density Studies

Although it is well known that 3D printing can produce near-net shapes, when developing a new part, the materials and process parameters influence the surface roughness. This determines whether the part must be machined. For the printed parts to look good and function properly, they must have a good surface finish with low surface roughness. If the surface roughness is high, for example, the printed part may experience high friction and wear rate when it comes into contact with another part that involves relative motion. Furthermore, a part with a high surface roughness is more likely to crack than apart with a better surface finish [35]. Layered structure formation, which contributes to surface roughness, is a common quality issue in FDM printed parts. Surface defects are unavoidable due to the printing process's fundamental principle, and the part has a high surface roughness due to the staircase or ridging effect. On inclined surfaces and corners, the staircase effect is quite visible, whereas the ridging effect is visible on flat surfaces when each layer deposited creates a minor bulge. Although there are several other methods for reducing or eliminating such effects, the cost is simply increased. The effect of CNT on composite surface roughness was studied, and the results are shown in Fig. 4. The average height deviations (Ra) measured on printed samples are used as a surface roughness parameter. As a result, the lower the value of Ra, the better the surface finish, with surface roughness in the range of 0.5 to 1.0 µm [36] for precision applications. As shown in the figure, the surface roughness of all samples, regardless of CNT content, was in the range of 0.477 µm to 0.707 µm. According to these values, the Ra decreases as the CNT content increases. The unreinforced HDPE produced the highest surface roughness value of 0.707 µm. In comparison to Ref [13], which reported an HDPE value of 11.37 µm, this value is significantly lower. Although a direct comparison with this reference is not possible due to process parameters, it highlights the suitability of the parameters chosen in this work to achieve minimal surface roughness in neat HDPE.

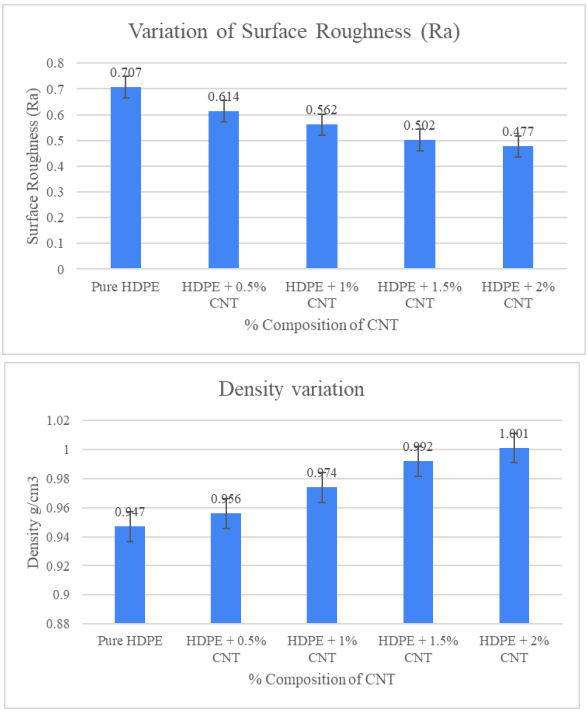

Fig. 4. a) Variation of surface roughness of HDPE with reinforcement of CNT b) Variation of density of HDPE with CNT

With the addition of 0.5% CNT, the surface roughness value was reduced to 0.614 µm. When compared to neat HDPE, surface roughness was reduced by approximately 13.15%. The reduction was minor, but it represents a significant improvement in surface finish. As more CNTs were added, the surface roughness value decreased, reaching a low of 0.477 µm for the HDPE/2.0%CNT composite. When compared to neat HDPE, the Ra value was reduced by approximately 48.2%. This finding differs significantly from previous research, which found that the addition of CNTs increased the surface roughness of composites. The work reported by Ref [24] revealed that the addition of CNTs increased the surface roughness of PLA composites. The Ra value of neat PLA increased from 5.5 µm to 16.5 µm for the PLA/3%CNT composite. Similarly, Mohapatra et al [37] found that adding functionalized CNT and ZnO to PLA composite increased surface roughness. An atomic force microscope surface topography analysis revealed a value of 200 nm for neat PLA

[DOI: 10.22068/ijmse.3231]

and a value of 480 nm for composite. The formation of agglomeration due to the van der Waals force between CNTs was the primary cause of the increase in surface roughness of composites with CNT addition [38]. However, some research has shown that adding CNTs reduces surface roughness [39, 40]. When compared to their respective unreinforced counterparts, MWCNT/aromatic polyamide [39] demonstrated a decrease in surface roughness at higher CNT concentrations, while CNT/epoxy composite [40] demonstrated a decrease at lower CNT concentrations. CNTs are well known for their high thermal conductivity, which may aid in the uniform cooling of the composite after printing. Although HDPE has been known to shrink and warp during the printing process, the addition of filler materials has helped it overcome these drawbacks. However, dispersion and filler content are critical because agglomeration can be detrimental to warpage reduction. The addition and increase in CNT content significantly impedes volumetric change in HDPE polymer chains. Because the CNTs have a very high interfacial surface area and are uniformly distributed in the HDPE matrix, shrinkage is greatly reduced. Furthermore, CNTs may reduce thermal gradients that occur during printing, allowing the composite to cool more uniformly [41]. This, in turn, aids in the elimination of dimensional inaccuracies such as warpages or surface irregularities, resulting in composites with lower surface roughness values. ASTM D792-13 standard was implemented for the measurement density of the developed novel polymer nanocomposite. The variation in density for the varied proportion of CNT to the polymer is shown in Figs. 4 (b). Pure HDPE had a density of 0.947 g/cm3 whereas HDPE + 2% CNT had a density of 1.001 g/cm3. There is an increment of 5.7 % in density on adding 2 weight % CNT in HDPE, which is a small amount in comparison to pure HDPE. The formation of interlayer between the molecules of polymer and CNT, homogenous dispersion of CNT in HDPE and no formation of any agglomerates lead to the increment in density of the developed nanocomposites

3.3. Impact Behaviour

Impact testing was performed on FDM 3D printed HDPE/CNT composites in order to better understand their response when subjected to localised impact loading. Few studies have been conducted on the impact responses of HDPE composites with varying CNT content, such as the effect of impact loading and the ability to dissipate the imparted kinetic energy. The impact response of HDPE composites will be determined by the matrix, CNT, the interphase region between HDPE and CNT, and printing parameters when compared to neat parts. All these constituents' mechanical properties will determine how the composites deform or fracture. Because the printing parameters for all HDPE composites are the same regardless of CNT content, the emphasis will be on determining how CNTs affect the impact behaviour of the HDPE matrix. The impact strength of neat HDPE and its CNT-reinforced composites is depicted in Fig. 5.

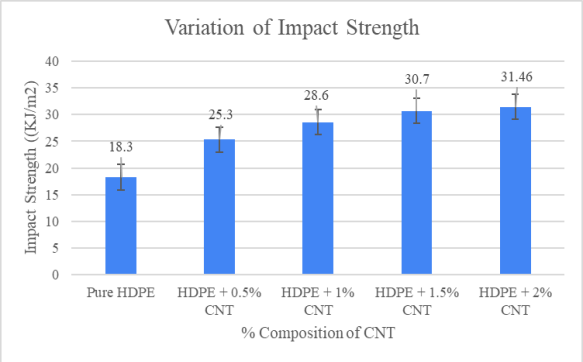

Fig. 5. Variation of Impact strength of HDPE with CNT reinforcement

The general trend indicates that as CNT content increases, impact strength values for HDPE tend to rise. The impact strength of neat HDPE was 18.3 KJ/m2, but with 0.5% CNT added, the strength increased to 25.3 KJ/m2. As a result, the addition of CNT increased the composite's impact energy-absorbing capacity by 38%, which is a significant improvement. Similarly, the impact strength values for the other HDPE composites with CNT content of 1.0%, 1.5%, and 2.0% were 28.6, 30.7, and 31.4 KJ/m2, respectively. The highest value obtained was for the HDPE/2.0%CNT composite, which is nearly 71.6% higher than neat HDPE. The interaction of CNTs with the HDPE matrix is the primary cause of the increase in impact strength. CNTs have good interfacial bonding with the HDPE matrix and are uniformly dispersed in it, as evidenced by the microstructural pieces of evidence shown in Fig. 3. Because of the aromatic nature of their

[DOI: 10.22068/ijmse.3231]

bonds, the atoms on the walls of CNTs are well-known to be highly stable. As a result, CNTs are mostly inert in nature, but when combined with a polymer matrix, they can interact via van der Waals interactions. As a result, there is poor load transfer across the CNT/matrix interface, and increasing the content results in heavy entangled bundles of CNT, which has a negative effect on mechanical properties. Furthermore, due to their extremely small size, high aspect ratio (as high as 1000), and high surface area, the CNTs are held together in such a way that they tend to form bundles. They are extremely difficult to disperse in polymer matrices due to this entanglement. To address these issues, the CNTs were first mixed with HDPE in a magnetic stirrer to disentangle them. CNTs peel away from the surface of individual agglomerates due to the vigorous stirring, dispersing them on the HDPE particles individually. Individual CNTs were uniformly dispersed in the HDPE, and the matrix completely covered them, leaving no gap at the interface, as seen in the micrographs (see Fig. 3). The primary reason for using a magnetic stirrer instead of ultrasonication or ball milling was to protect the CNTs. Previous studies [42, 43] found that long-term ultrasonication caused localised damage or the formation of defects such as disordered sp3 carbon. As a result, even if cracks form elsewhere in the sample, the CNTs prevent them from spreading. The probability of crack arrest increases as CNT content increases, allowing the sample to absorb more energy and thus increasing impact strength. Little attention has been paid to the effect of carbon nanotubes on the impact strength of FDM printed composites. Pan et al [33], for example, discovered that using CNT as a filler material reduced the impact strength of polyphenylene sulphide composites marginally. The addition of CNTs increased the crystallinity of the composites, causing them to become brittle. In a similar study, Vidakis et al [44] reported a decrease in impact strength of polyamide 12 composites after the addition of CNTs. CNTs made the composites more brittle, allowing them to absorb less impact energy, which resulted in a decrease in strength values. CNTs were unable to increase the impact strength of various polymer composites, particularly those created using 3D printing. According to these studies, adding CNT to composites makes them stiffer and brittle, rendering them unable to withstand impact loading. It is worth noting that none of these studies identified CNT-related defect generation as the primary cause of the drop in impact strength. Because of agglomeration or poor matrix bonding, CNTs are prone to increasing defect density. When the mixing and printing process parameters are not optimised, such flaws occur frequently. The impact strength of composites is also harmed in such cases because these defects act as crack initiators in the composites. This is not to say that carbon nanotubes have a negative impact on the energy-absorbing capacity of polymer composites. When Ghoshal et al [45] investigated carbon nanotube-reinforced polypropylene, they discovered that as the CNT content increased, so did the strength. It is worth noting that adding 1.0% CNT by weight increased the impact strength of polypropylene by 152%. The coherent and long interfaces between polypropylene and CNTs, as well as the small spherulite size, were the primary reasons for the increased strength. Laurenzi et al. [46] thoroughly documented the role of the interface in improving the impact strength of Kevlar 29 epoxy/CNTs composites. The composites had strong covalent bonding between CNTs and polymeric chains, which significantly increased the impact strength. As a result, it is impossible to predict whether the addition of CNTs will increase or decrease the impact energy absorbing capacity of polymeric composites; rather, it is dependent on several other factors such as material composition, CNT surface condition, and printing parameters. Nonetheless, the results of this study showed that increasing CNT content increased impact strength due to improved interfacial bonding and uniform dispersion in the HDPE matrix.

3.4. *Tensile properties*

Understanding the effect of CNTs on the tensile behaviour of HDPE composites is critical for structural applications. The effect of CNT content on the tensile strength and Young's modulus of HDPE composites was studied, and the results are shown in Figs. 6 (a) and (b). The tensile strength and Young's modulus of HDPE were also determined under comparable testing conditions for comparison purposes. The tensile strength of HDPE increased with increasing CNT content (see Fig. 6 (a)). The pure HDPE has a tensile strength of 26.4 MPa, according to the tensile test. The addition of 0.5% CNT increased HDPE

[DOI: 10.22068/ijmse.3231]

composite tensile strength to 27.4 MPa. In contrast to impact strength, the increase in strength (3.8%) here is quite minor. As the CNT content increased from 0.5% to 2.0%, the tensile strength increased from 27.4 MPa to 33.1 MPa.

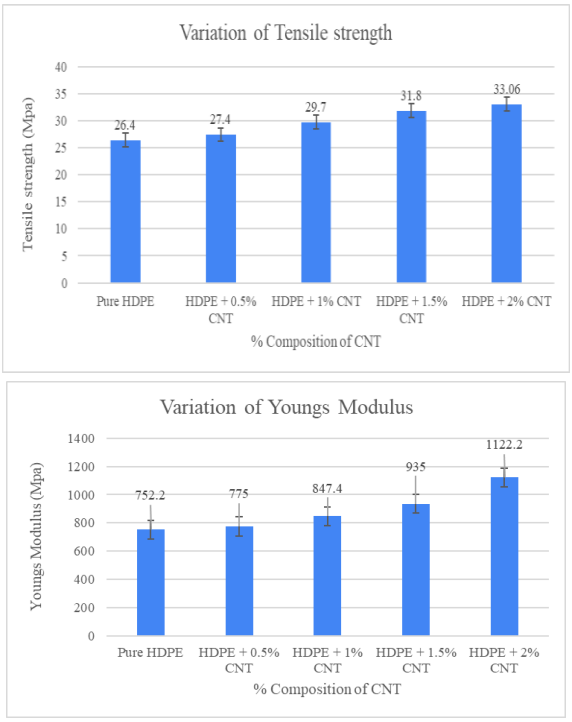

Fig. 6. a) Variation of Tensile strength of HDPE with CNT reinforcement b) Variation of Youngs modulus of HDPE with CNT reinforcement

This implies that CNTs are effective at increasing tensile strength. When compared to neat HDPE, the HDPE/2.0%CNT composite increased strength by approximately 25.4%. The Young's modulus of HDPE and CNT-reinforced composites is depicted in Fig. 6b. The value of 752.2 MPa for neat HDPE was increased to 775 MPa with the addition of 0.5% CNT. The addition of CNT increased the Young's modulus by about 3%, which is a small increase. As the CNT content increased from 0.5% to 2.0%, the modulus increased from 775 MPa to 1122.2 MPa. The modulus of the HDPE/2.0%CNT composite increased by approximately 49.2% when compared to pure HDPE. When CNT content is 2%, modulus increases significantly. CNTs are primarily responsible for increasing HDPE composite modulus and strength. The influence extends not only to the microstructure or properties of the sample but also to the printing parameters used in sample fabrication. It is well understood that the properties of FDM printing are determined by the bonding between the layers, the density of pores, and the strength of the individual constituents of the composite. CNT content, dispersion, orientation, and matrix bonding are all important filler properties. Various parameters can have varying effects on the quality of the final sample during the extrusion and printing processes. The melt flow rate is high due to the low viscosity of pure HDPE, resulting in the formation of a wider extrudate that degrades the surface quality of the printed sample. The addition of CNTs to polymer matrices, on the other hand, can have a variety of effects on the viscosity and flow rate of the melt. The addition of CNTs has decreased the melt flow rate in some cases due to the nucleation effect between CNT and polymer matrix [29, 47]. As a result, the activation energy required for viscous flow increased. However, in this case, the CNT concentration is quite optimal, and if they are dispersed individually, their influence on the viscosity may not be significant enough to cause under-flow. The increase in viscosity could be due to hydrodynamic interactions rather than CNT-CNT interactions. Even if some CNT agglomerates remain in the composite filament, they are broken down by the hydrodynamic forces in the melt during the printing process, and the converging flow at the nozzle ensures better CNT alignment [47]. The alignment of CNTs in the printing direction may be caused by a combination of the extrusion process and hydrodynamic forces. This is beneficial because a higher melt flow rate improves composite fabrication efficiency and surface quality. Furthermore, the increased melt flow rate reduces the likelihood of void formation between roads/rasters. Road-to-road adhesion will be poor if flow-induced aggregation and modification of CNT orientation occur during extrusion or printing. According to Rinaldi et al. [48], when the CNT content exceeded 3%, the tensile strength and modulus of composites in filament and printed states decreased significantly. Property degradation was attributed to poor adhesion between filaments within the layer and partial agglomeration of CNTs. Furthermore, it is well known that carbon nanotubes have extremely high strength and elastic modulus. Because of their exceptional properties, carbon nanotubes improve the tensile strength of HDPE. However,

[DOI: 10.22068/ijmse.3231]

increasing strength requires more than just incorporating CNTs; it also requires ensuring their uniform dispersion and strong interfacial bonding with the HDPE matrix. The composites had uniform CNT distribution, as seen in the SEM micrographs (Fig. 3). The absence of agglomerations in the matrix reduces the number of stress concentrators dramatically. Despite the higher CNT concentration, the uniform dispersion allows a larger surface area of the filler to interact with the HDPE matrix, maximising the filler's influence on the tensile properties. Furthermore, the lack of a gap at the interface and improved HDPE coverage of the CNT surface resulted in strong, stress-free regions for improved load transfer between CNT and HDPE. The load transfer from HDPE to CNT becomes more efficient as the number of CNTs increases, which is the primary cause of the high tensile strength and modulus of composites with a high CNT content of 2%. Polymer composites' tensile properties can increase or decrease depending on dispersion and bonding.

Bortoli et al. [49] investigated the tensile properties of PLA composites using two different CNTs, commercial purity and functionalized CNTs. The tensile strength and elastic modulus of composites containing commercial purity CNTs decreased due to poor dispersion, whereas those containing functionalized CNTs exhibited enhanced properties due to improved matrix-filler interaction. CNTs improved the tensile strength and modulus of HDPE composites overall.

3.5. Fracture Analysis

SEM analysis of fracture samples was performed to better understand the fracture mechanism after a tensile test, and the results are shown in Fig. 7 (a) (h). The fracture surface of pure HDPE exhibits ductile failure, as shown in Figs. 7 (a) and (b).

The characteristics of HDPE undergoing plastic deformation are visible on the fractured surface. In general, HDPE fails to ductile with significant plastic deformation in the form of extensive necking [50]. However, due to the presence of defects in the deposited filament, the deformation process in this case is quite different. A closer look at the HDPE revealed the presence of small voids with a diameter of about 10 m (see Fig. 7 (b)). On the fracture surface, triangular inter-filament pores were discovered. The filaments at the top and bottom were not touching with a positive air gap, indicating incomplete neck growth. Because the filaments solidify prior to the completion of the coalescence process, 100% coalescence between adjacent filaments is not possible in ideal FDM printing conditions. These are some of the reasons why the HDPE sample had the lowest tensile strength and the least amount of necking.

Figs. 7 (c) and (d) show brittle fracture surfaces for HDPE composites containing 0.5% and 1.0% CNT. The relatively smooth fractured surface is an important feature of brittle failure. CNTs occupy the free positions in the polymeric chains, and their tendency to restrict chain mobility causes HDPE to lose ductility and begin to behave brittlely. Vidakis et al. [51] reported similar findings in their work on FFF-printed HDPE/TiO_2 nanocomposites. Because TiO_2 particles occupied free positions in HDPE polymer chains, the composites failed in a less ductile manner. Furthermore, the surfaces of both composites showed individual CNTs with no agglomeration. This backs up the previous discussion about CNT alignment in the HDPE matrix during the extrusion and printing processes. There were no entangled CNT structures in any of the fractured regions, only dispersed CNTs that were effective at transferring loads from HDPE to them. However, the triangular pores were found to be shrinking in these cases, indicating that the addition of CNTs increased the melt flow rate. Figs. 7 (g) and (h) show the fracture surfaces of HDPE composites containing 2.0% CNT, which also had a smooth surface, indicating brittle failure. The presence of HDPE remnants on the CNT surface indicates the strength of their interfacial bonding. This is the main reason that no fracture regions showed CNT pull-out. No composite, regardless of CNT content, showed filament or layer failure, indicating excellent adhesion.

4. CONCLUSIONS

In this work, HDPE/CNT composites were developed using twin screw extrusion and FDM 3D printing processes. The effect of the addition of CNTs in varying weight percentages to the HDPE matrix was evaluated by conducting microstructural, surface roughness, impact, and tensile studies.

[DOI: 10.22068/ijmse.3231]

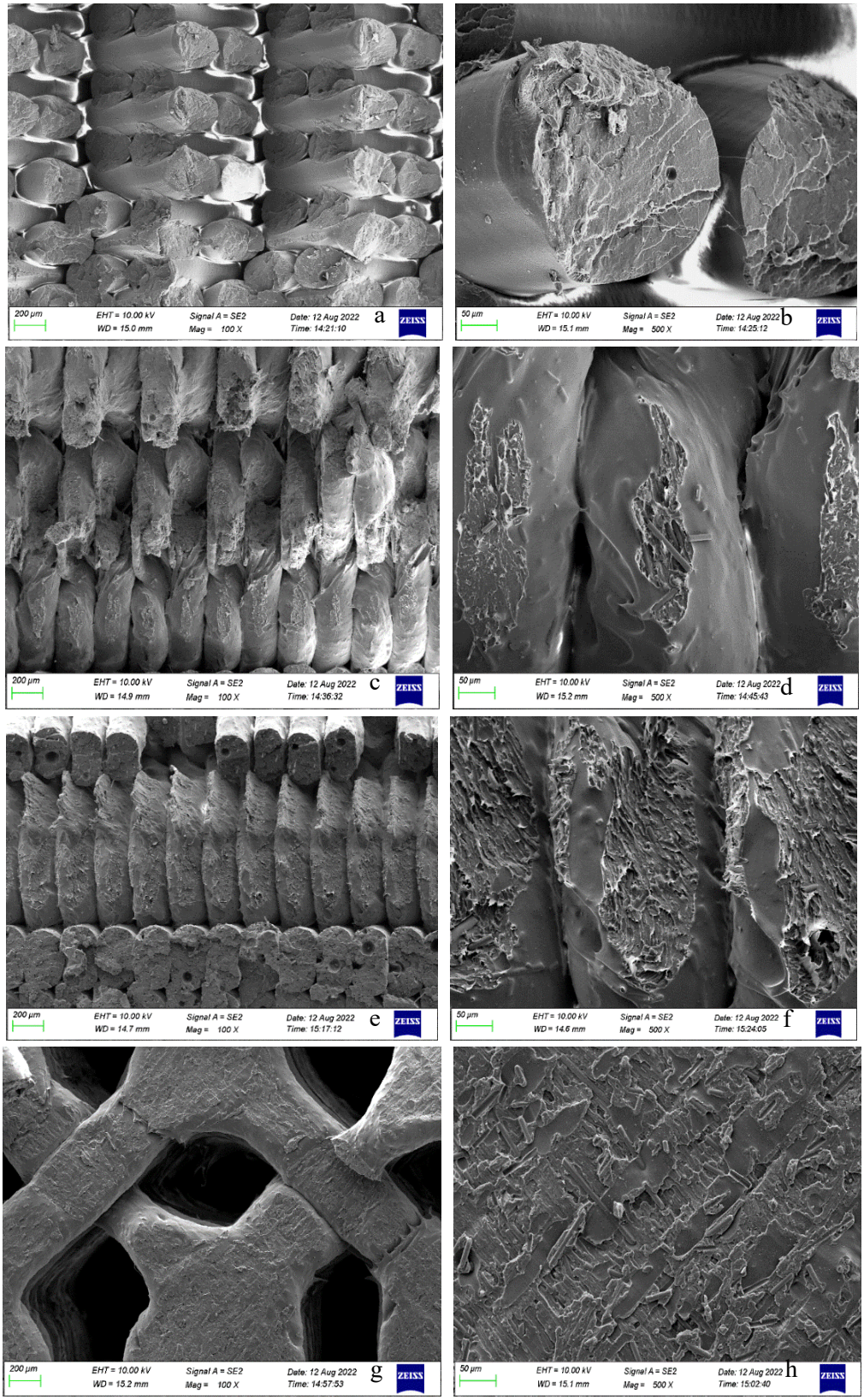

Fig. 7. SEM micrographs of fractured samples a,b) 0.5%, c,d) 1.0%, e,f) 1.5% and g,h) 2.0% CNT reinforced HDPE composites

[DOI: 10.22068/ijmse.3231]

1. Microstructure analysis using SEM showed uniform dispersion of CNTs and with the increase in CNT content revealed no agglomeration. The interfacial bonding between CNT and HDPE matrix was found to be continuous and free from defects.
2. Surface roughness studies showed a decrease in R_a value as the CNT content was increased in the HDPE composites. The lowest surface roughness was recorded for the HDPE/2.0%CNT composite. The reduction in volumetric change in HDPE polymer chains and diminishing of thermal gradients due to the presence of CNTs helped the composites to overcome the dimensional inaccuracy-related issues which in turn resulted in lower surface roughness values for composites.
3. The HDPE composites showed an increase in impact and tensile strength with the increase in CNT content. The better dispersion and good interfacial bonding of CNTs with the HDPE matrix helped the composite to bear higher loads. The HDPE/2.0%CNT composite was among the best when compared to neat HDPE in terms of increase in impact and tensile strength by approximately 71.6% and 25.4%, respectively The elastic modulus was also found to increase with CNT content with HDPE/2.0%CNT composite showing highest value of 1122.2 Mpa with an increase of 49 % from pure HDPE.
4. The fracture analysis using SEM showed the brittle type of failure for all composites while neat HDPE showed ductile fracture. The fracture surface analysis did support the claims of uniform dispersion and alignment of CNTs in the printing direction.

REFERENCES

[1]. HR, Mohankumar, Maha Gundappa M. Benal, Pradeepkumar GS, Vijay Tambrallimath, Keshavamurthy Ramaiah, TM Yunus Khan, Javed Khan Bhutto, and Mohammed Azam Ali. "Effect of Short Glass Fiber Addition on Flexural and Impact Behavior of 3D Printed Polymer Composites." ACS omega, 2023, 8, 9212-9220.

[2]. Tambrallimath, Vijay, R. Keshavamurthy, Saravana D. Bavan, Arun Y. Patil, T. M. Yunus Khan, Irfan Anjum Badruddin, and Sarfaraz Kamangar. "Mechanical properties of PC-ABS-based graphene-reinforced polymer nanocomposites fabricated by FDM process." Polymers, 2021, 13, 2951.

[3]. Gao, Wei, Yunbo Zhang, Devarajan Ramanujan, Karthik Ramani, Yong Chen, Christopher B. Williams, Charlie CL Wang, Yung C. Shin, Song Zhang, and Pablo D. Zavattieri. "The status, challenges, and future of additive manufacturing in engineering." Computer-Aided Design, 2015, 69, 65-89.

[4]. Bilkar, Digamba, R. Keshavamurthy, and Vijay Tambrallimath. "Influence of carbon nanofiber reinforcement on mechanical properties of polymer composites developed by FDM." Materials Today Proceedings, Int. Con. on Advances in Materials and Manufacturing Applications. (IConAMMA 2019), Karnataka, India, 2019, 1757-1760.

[5]. Ngo, Tuan D., Alireza Kashani, Gabriele Imbalzano, Kate TQ Nguyen, and David Hui. "Additive manufacturing (3D printing): A review of materials, methods, applications and challenges." Composites Part B: Engineering, 2018, 143, 172-196.

[6]. Tofail, Syed AM, Elias P. Koumoulos, Amit Bandyopadhyay, Susmita Bose, Lisa O'Donoghue, and Costas Charitidis. "Additive manufacturing: scientific and technological challenges, market uptake and opportunities." Materials today, 2018, 21, 22-37.

[7]. Tambrallimath, Vijay, R. Keshavamurthy, Paulo Davim, GS Pradeep Kumar, Gloria Pignatta, Abhinandan Badari, TM Yunus Khan, and Irfan Anjum Badruddin. "Synthesis and characterization of flyash reinforced polymer composites developed by Fused Filament Fabrication." Journal of materials research and technology, 2022, 21, 810-826.

[8]. Tambrallimath, Vijay, R. Keshavamurthy, Arun Patil, and H. Adarsha. "Mechanical and tribological characteristics of polymer composites developed by fused filament fabrication." Fused Deposition Modeling Based 3D Printing, 2021, 151-166.

[9]. Dizon, John Ryan C., Alejandro H. Espera Jr, Qiyi Chen, and Rigoberto C. Advincula. "Mechanical characterization of 3D-printed polymers." Additive manufacturing, 2018,

[DOI: 10.22068/ijmse.3231]

20, 44-67.
[10]. Daminabo, Samuel Clinton, Saurav Goel, Sotirios A. Grammatikos, Hamed Yazdani Nezhad, and Vijay Kumar Thakur. "Fused deposition modeling-based additive manufacturing (3D printing): techniques for polymer material systems." Materials today chemistry, 2020, 16, 100248.
[11]. Tambrallimath, Vijay, R. Keshavamurthy, D. Saravanabavan, Praveennath G. Koppad, and GS Pradeep Kumar. "Thermal behavior of PC-ABS based graphene filled polymer nanocomposite synthesized by FDM process." Composites Communications, 2019, 15, 129-134.
[12]. Mostafa, Khaled G., Carlo Montemagno, and Ahmed Jawad Qureshi. "Strength to cost ratio analysis of FDM Nylon 12 3D Printed Parts." Procedia Manufacturing, 2018, 26, 753-762.
[13]. K. Szykiedans, W. Credo, D. Osinski, Selected mechanical properties of PETG 3-D prints, Procedia Engineering, 2017, 177, 455-461.
[14]. Samykano, M. "Mechanical property and prediction model for FDM-3D printed polylactic acid (PLA)." Arabian Journal for Science and Engineering, 2021, 46, 7875-7892.
[15]. Chanda, Manas, and Salil K. Roy. Industrial polymers, specialty polymers, and their applications, 2008, Vol. 74. CRC press.
[16]. Schirmeister, Carl G., Timo Hees, Erik H. Licht, and Rolf Mülhaupt. "3D printing of high density polyethylene by fused filament fabrication." Additive Manufacturing, 2019, 28, 152-159.
[17]. Chong, Siewhui, Guan-Ting Pan, Mohammad Khalid, Thomas C-K. Yang, Shuo-Ting Hung, and Chao-Ming Huang. "Physical characterization and pre-assessment of recycled high-density polyethylene as 3D printing material." Journal of Polymers and the Environment, 2017, 25, 136-145.
[18]. Gudadhe, Aniket, Nirmalya Bachhar, Anil Kumar, Prem Andrade, and Guruswamy Kumaraswamy. "Three-dimensional printing with waste high-density polyethylene." ACS Applied Polymer Materials, 2019, 1, 3157-3164.
[19]. S. Kumar, R. Singh, T. Singh, A. Batish, "On investigation of rheological, mechanical and morphological characteristics of waste polymer-based feedstock filament for 3D printing applications." Journal of Thermoplastic Composite Materials, 2021, 34, 902-928.
[20]. M.F. Yu, O. Lourie, M.J. Dyer, K. Moloni, T.F. Kelly, R.S. Ruoff, "Strength and breaking mechanism of multiwalled carbon nanotubes under tensile load." Science, 2000, 287, 637-640.
[21]. Kim, Hyung-ick, Mei Wang, Stephanie K. Lee, Junmo Kang, Jae-Do Nam, Lijie Ci, and Jonghwan Suhr. "Tensile properties of millimeter-long multi-walled carbon nanotubes." Scientific reports, 2017, 7, 9512.
[22]. Koppad, Praveennath G., Vikas Kumar Singh, C. S. Ramesh, Ravikiran G. Koppad, and K. T. Kashyap. "Metal matrix nanocomposites reinforced with carbon nanotubes." Advanced carbon materials and technology, 2014, Ch 9, 331-376.
[23]. Kashyap, K. T., Praveennath G. Koppad, K. B. Puneeth, HR Aniruddha Ram, and H. M. Mallikarjuna. "Elastic modulus of multiwalled carbon nanotubes reinforced aluminium matrix nanocomposite–A theoretical approach." Computational materials science, 2011, 50, 2493-2495.
[24]. Spitalsky, Zdenko, Dimitrios Tasis, Konstantinos Papagelis, and Costas Galiotis. "Carbon nanotube–polymer composites: chemistry, processing, mechanical and electrical properties." Progress in polymer science, 2010, 35, 357-401.
[25]. Tarfaoui, Mostapha, Khalid Lafdi, and Ahmed El Moumen. "Mechanical properties of carbon nanotubes based polymer composites." Composites Part B: Engineering, 2016, 103, 113-121.
[26]. Jouni, Mohammad, David Djurado, Valérie Massardier, and Gisèle Boiteux. "A representative and comprehensive review of the electrical and thermal properties of polymer composites with carbon nanotube and other nanoparticle fillers." Polymer International, 2017, 66, 1237-1251.
[27]. Ye, Wenli, Wenzheng Wu, Xue Hu, Guoqiang Lin, Jinyu Guo, Han Qu, and Ji Zhao. "3D printing of carbon nanotubes

[DOI: 10.22068/ijmse.3231]

reinforced thermoplastic polyimide composites with controllable mechanical and electrical performance." Composites Science and Technology, 2019, 182, 107671.

[28]. Sezer, H. Kürşad, and Oğulcan Eren. "FDM 3D printing of MWCNT re-inforced ABS nano-composite parts with enhanced mechanical and electrical properties." Journal of Manufacturing Processes, 2019, 37, 339-347.

[29]. Yang, Leipeng, Shujuan Li, Xing Zhou, Jia Liu, Yan Li, Mingshun Yang, Qilong Yuan, and Wei Zhang. "Effects of carbon nanotube on the thermal, mechanical, and electrical properties of PLA/CNT printed parts in the FDM process." Synthetic Metals, 2019, 253, 122-130.

[30]. Zhou, Xing, Jingrui Deng, Changqing Fang, Wanqing Lei, Yonghua Song, Zisen Zhang, Zhigang Huang, and Yan Li. "Additive manufacturing of CNTs/PLA composites and the correlation between microstructure and functional properties." Journal of Materials Science & Technology, 2021, 60, 27-34.

[31]. Nadernezhad, Ali, Serkan Unal, Navid Khani, and Bahattin Koc. "Material extrusion-based additive manufacturing of structurally controlled poly (lactic acid)/carbon nanotube nanocomposites." The International Journal of Advanced Manufacturing Technology, 2019, 102, 2119-2132.

[32]. Gonçalves, Carolina, Inês C. Gonçalves, Fernão D. Magalhães, and Artur M. Pinto. "Poly (lactic acid) composites containing carbon-based nanomaterials: A review." Polymers, 2017, 9, 269.

[33]. Pan, Shengyou, Hongyao Shen, and Linchu Zhang. "Effect of carbon nanotube on thermal, tribological and mechanical properties of 3D printing polyphenylene sulfide." Additive Manufacturing, 2021, 47, 102247.

[34]. Vidakis, Nectarios, Markos Petousis, Emmanouil Velidakis, Lazaros Tzounis, Nikolaos Mountakis, Orsa Boura, and Sotirios A. Grammatikos. "Multi-functional polyamide 12 (PA12)/multiwall carbon nanotube 3D printed nanocomposites with enhanced mechanical and electrical properties." Advanced Composite Materials, 2022, 31, 630-654.

[35]. Chand, Ramesh, Vishal S. Sharma, Rajeev Trehan, Munish Kumar Gupta, and Murat Sarikaya. "Investigating the dimensional accuracy and surface roughness for 3D printed parts using a multi-jet printer." Journal of Materials Engineering and Performance, 2023, 32, 1145-1159.

[36]. Zhong, Zhao-Wei. "Surface roughness of machined wood and advanced engineering materials and its prediction: a review." Advances in Mechanical Engineering, 2021, 13, 16878140211017632.

[37]. Mohapatra, Agneyarka, Nidhin Divakaran, Y. Alex, Ajay Kumar PV, and Smita Mohanty. "The significant role of CNT-ZnO core-shell nanostructures in the development of FDM-based 3D-printed triboelectric nanogenerators." Materials Today Nano, 2023, 22, 100313.

[38]. Stanciu, Nicoleta-Violeta, Felicia Stan, Catalin Fetecau, and Florin Susac. "On the Feasibility of Printing 3D Composite Objects Based on Polypropylene/Multi-Walled Carbon Nanotubes." In MATEC Web of Conferences, EDP Sciences, 2019, vol. 290, p. 03017.

[39]. Shawky, Hosam A., So-Ryong Chae, Shihong Lin, and Mark R. Wiesner. "Synthesis and characterization of a carbon nanotube/polymer nanocomposite membrane for water treatment." Desalination, 2011, 272, 46-50.

[40]. Kim, Hyehee, Sen Gao, Sanghyun Hong, Pyoung-Chan Lee, Young Lae Kim, Jin Uk Ha, Sun Kyoung Jeoung, and Yung Joon Jung. "Multifunctional primer film made from percolation enhanced CNT/Epoxy nanocomposite and ultrathin CNT network." Composites Part B: Engineering, 2019, 175, 107107.

[41]. Spoerk, Martin, Clemens Holzer, and Joamin Gonzalez-Gutierrez. "Material extrusion-based additive manufacturing of polypropylene: A review on how to improve dimensional inaccuracy and warpage." Journal of Applied Polymer Science, 2020, 137, 48545.

[42]. Lu, K., R. Lago, Y. Chen, M. Green, P. Harris, and S. Tsang. "Mechanical damage of carbon nanotubes by ultrasound."

[DOI: 10.22068/ijmse.3231]

Carbon, 1996, 34, 6, 814-816.
[43]. Ma, Peng-Cheng, Naveed A. Siddiqui, Gad Marom, and Jang-Kyo Kim. "Dispersion and functionalization of carbon nanotubes for polymer-based nanocomposites: A review." Composites Part A: Applied Science and Manufacturing, 2010, 41, 1345-1367.
[44]. Vidakis, Nectarios, Markos Petousis, Lazaros Tzounis, Emmanuel Velidakis, Nikolaos Mountakis, and Sotirios A. Grammatikos. "Polyamide 12/multiwalled carbon nanotube and carbon black nanocomposites manufactured by 3D printing fused filament fabrication: A comparison of the electrical, thermoelectric, and mechanical properties." C, 2021, 7, 38.
[45]. Ghoshal, Sushanta, Po-Hsiang Wang, Prabhakar Gulgunje, Nikhil Verghese, and Satish Kumar. "High impact strength polypropylene containing carbon nanotubes." Polymer, 2016, 100, 259-274.
[46]. Laurenzi, S., R. Pastore, G. Giannini, and M. Marchetti. "Experimental study of impact resistance in multi-walled carbon nanotube reinforced epoxy." Composite Structures, 2013, 99, 62-68.
[47]. Patanwala, Huseini S., Danting Hong, Sahil R. Vora, Brice Bognet, and Anson WK Ma. "The microstructure and mechanical properties of 3D printed carbon nanotube-polylactic acid composites." Polymer Composites, 2018, 39, E1060-E1071.
[48]. Rinaldi, Marianna, Mario Bragaglia, and Francesca Nanni. "Mechanical performance of 3D printed polyether-ether-ketone nanocomposites: An experimental and analytic approach." Composite Structures, 2023, 305, 116459.
[49]. De Bortoli, L. S., R. De Farias, D. Z. Mezalira, L. M. Schabbach, and M. C. Fredel. "Functionalized carbon nanotubes for 3D-printed PLA-nanocomposites: Effects on thermal and mechanical properties." Materials Today Communications, 2022, 31, 103402.
[50]. Kwon, H. J., and P-YB Jar. "Toughness of high-density polyethylene in plane-strain fracture." Polymer Engineering & Science, 2006, 46, 1428-1432.
[51]. Vidakis, Nectarios, Markos Petousis, Athena Maniadi, Vassilis Papadakis, and Alexandra Manousaki. "MEX 3D printed HDPE/TiO2 nanocomposites physical and mechanical properties investigation." Journal of Composites Science, 2022, 6, 209.

[DOI: 10.22068/ijmse.3231]